International Journal of Control, Automation and Systems 17(5) (2019) 1167-1176
http://dx.doi.org/10.1007/s12555-018-0499-6
ISSN:1598-6446 eISSN:2005-4092
http://www.springer.com/12555

An Improved Consistent Subspace Identification Method Using Parity Space for State-space Models

Jie Hou*, Fengwei Chen, Penghua Li, Zhiqin Zhu, and Fei Liu

Abstract: In this paper, an alternative consistent subspace identification method using parity space is proposed. The future/past input data and the past output data are used to construct the instrument variable to eliminate the noise effect on consistent estimation. The extended observability matrix and the triangular block-Toeplitz matrix are then retrieved from a parity space of the noise-free matrix using a singular value decomposition based method. The system matrices are finally estimated from the above estimated matrices. The consistency of the proposed method for estimation of the extended observability matrix and the triangular block-Toeplitz matrix is established. Compared with the classical SIMs using parity space like SIMPCA and SIMPCA-Wc, the proposed method generally enhances the estimated model efficiency/accuracy thanks to the use of future input data. Two examples are presented to illustrate the effectiveness and merit of the proposed method.

Keywords: Consistency, instrumental variables, parity space, rank condition, subspace identification.

1. INTRODUCTION

Subspace identification methods (SIMs) have been known as very useful tools for state-space systems, which have been attracted considerable attention [1–3] in the past decades. The main proponents of these methods are MOESP (Multivariate Output Error State-space) proposed in [4], N4SID (Numerical algorithms for State-space SubSpace IDentification) in [5], and CVA (Canonical Variate Analysis) in [6]. The statistical properties of these methods are fairly well established in a series of papers [7–10]. The above-mentioned methods estimate the extended observability matrix or state from a signal subspace of certain noise-free matrix, then retrieve the system matrices based on the above intermediate results.

In parallel, owing to that the SIMs using parity space like SIMPCA [11, 12] and SIMPCA-Wc [13], can estimate the extended observability matrix and the triangular block-Toeplitz matrix simultaneously from the same parity space of the noise-free matrix, all of the system matrices can then be easily retrieved from the estimated matrices. These methods have gained great interest from both academy and industry in the recent years, and have been widely applied for system identification [14–20], process monitoring and fault diagnosis [21–25], and advanced control [26–30].

Note that the instrument variables (IVs) in SIMPCA and SIMPCA-Wc only contain the past input/output data, which are uncorrelated with the future input data for white input system, but are weakly correlated with the future input/output data for colored input system. This may lead to a loss in the rank of the future input/output Hankel matrix, thus SIMPCA and SIMPCA-Wc may yield biased solutions, especially, for white input systems.

To enhance the estimation efficiency/accuracy for SIMPCA and SIMPCA-Wc, an improvd consistent parity-space based SIM using a new IV is proposed in the same framework of SIMPCA and SIMPCA-Wc. The novelty of the new IV lies in that it includes not only the past input and output data as used in SIMPCA and SIMPCA-Wc, but also the future input data, which can eliminate the noise effect from the future input/output Hankel matrix without causing a loss in the rank of the future input/output Hankel matrix. After that, the proposed method provides consis-

Manuscript received July 19, 2018; revised November 21, 2018 and December 28, 2018; accepted January 2, 2019. Recommended by Associate Editor Yongping Pan under the direction of Editor Jay H. Lee. This research was supported by the National Natural Science Foundation of China under Grant 61803061, 61703347, and 61703311; Science and Technology Research Program of Chongqing Municipal Education Commission grant KJQN201800603; the Chongqing Natural Science Foundation Grant cstc2018jcyjAX0167; the Common Key Technology Innovation Special of Key Industries of Chongqing science and Technology Commission under Grant cstc2017zdcy-zdyfX0067; the Artificial Intelligence Technology Innovation Significant Theme Special Project of Chongqing science and Technology Commission under Grant cstc2017rgzn-zdyfX0014 and cstc2017rgzn-zdyfX0035.

Jie Hou, Penghua Li, and Zhiqin Zhu are with the College of Automation, Chongqing University of Posts and Telecommunications, No. 2 Chongwen Road, Chongqing, China (e-mails: jiehou.phd@hotmail.com, liph@cqupt.edu.cn, zhuzq@cqupt.edu.cn). Fengwei Chen is with the Department of Automation, Wuhan University, No. 299 Bayi Road, Wuhan, Hubei, China (e-mail: fengwei.chen@outlook.com). Fei Liu is with the National Robot Test and Assessment Center (Chongqing), Chongqing Dexin Robot Testing Center Co., Ltd, No. 101 Yunhan Road, Liangjiang New Area, Chongqing, China (e-mail: liufei299@yahoo.com).
* Corresponding author.

tent estimates, and this explains the reason why the new method enhances the estimation efficiency/accuracy. Note that the proposed method can be easily extended to recursive real-time applications by the strategies in [31].

The remainder of the paper is organized as follows: In Section 2 the identification problem is briefly presented. In Section 3 the proposed SIM is presented in details, followed by the consistency analysis in Section 4. Illustrative examples are shown in Section 5 to demonstrate the effectiveness of the proposed method. Finally, conclusions are drawn in Section 6.

2. PROBLEM FORMULATION AND ASSUMPTION

Consider the following state-space model,

$$\begin{cases} x(t+1) = Ax(t) + Bu(t), \\ y(t) = Cx(t) + Du(t) + v(t), \end{cases} \tag{1}$$

where $x(t) \in \Re^{n_x}, u(t) \in \Re^{n_u}$, and $y(t) \in \Re^{n_y}$ are the state-vector, observed input signal, and observed output signal, respectively. The system is corrupted by measurement noise $v(t) \in \Re^{n_y}$. Denote by A,B,C,D the system matrices defined with compatible dimensions.

The following assumptions are made for identification.

Assumption 1: The eigenvalues of A lie inside the unit circle.

Assumption 2: The system is minimal in the sense that the pair (A,C) is observable and the pair (A,B) is reachable.

Assumption 3: The noise $v(t)$ is a stationary zero-mean Gaussian white noise, and it is uncorrelated with input signal.

The identification task is to estimate the system matrices (A,B,C,D) up to a similarity transformation.

Denote by p and f the past and future horizons ($p = f \geq n_x$ [1]). Define the past and future input Hankel matrices, respectively, by

$$U_p = \begin{bmatrix} u(t-p) & \dots & u(t-p+N-1) \\ u(t-p+1) & \dots & u(t-p+N) \\ \vdots & \ddots & \vdots \\ u(t-1) & \dots & u(t+N-2) \end{bmatrix}, \tag{2}$$

$$U_f = \begin{bmatrix} u(t) & \dots & u(t+N-1) \\ u(t-p+1) & \dots & u(t+N) \\ \vdots & \ddots & \vdots \\ u(t+f-1) & \dots & u(t+f+N-2) \end{bmatrix}. \tag{3}$$

Similar formulations are defined for Y_p, Y_f, V_p, and V_p.

The state sequences are defined as

$$X_p = [x(t-p), x(t-p+1), ..., x(t-p+N-1)], \tag{4}$$

$$X_f = [x(t), x(t+1), ..., x(t+N-1)]. \tag{5}$$

Based on the descriptiones in (1), an block-Hankel state-space model can be formulated as

$$X_f = A^p X_p + L_p U_p, \tag{6}$$

$$Y_p = \Gamma_p X_p + H_p U_p + V_p, \tag{7}$$

$$Y_f = \Gamma_f X_f + H_f U_f + V_f, \tag{8}$$

where the controllability matrix and observability matrix are, respectively, $L_f = [A^{f-1}B \dots B]$ and $\Gamma_f = [C^\top \dots (CA^{f-1})^\top]^\top$, and the triangular Toeplitz matrix is

$$H_f = \begin{bmatrix} D & \dots & \dots & 0 \\ CB & \dots & \dots & 0 \\ \vdots & \vdots & \ddots & \vdots \\ CA^{f-2} & \dots & CB & D \end{bmatrix}.$$

The matrices Γ_p and H_p are, respectively, defined similarly to Γ_f and H_f.

3. PROPOSED METHOD

3.1. Estimation of Γ_f and H_f

Introducing three short-hands $Z_p = [Y_p^\top U_p^\top]^\top$, $Z_f = [Y_f^\top U_f^\top]^\top$, and $Z = [Z_p^\top U_f^\top]^\top$, (7) can be rewritten in the state-space form

$$Z_f = \begin{bmatrix} \Gamma_f & H_f \\ 0 & I \end{bmatrix} \begin{bmatrix} X_f \\ U_f \end{bmatrix} + \begin{bmatrix} I \\ 0 \end{bmatrix} E_f. \tag{9}$$

Given that Z is highly correlated with $[X_f^\top U_f^\top]\top$, but uncorrelated to the noise term E_f. We use $Z^\top (ZZ^\top/N)^{-1/2}$ as IV to remove E_f from Z_f. By post-multiplying both sides of (9) with Z yields

$$\frac{Z_f Z^\top}{N} \left(\frac{ZZ^\top}{N}\right)^{-1/2} = \frac{1}{N} \left(\begin{bmatrix} \Gamma_f & H_f \\ 0 & I \end{bmatrix} \begin{bmatrix} X_f \\ U_f \end{bmatrix} + \begin{bmatrix} I \\ 0 \end{bmatrix} E_f \right) Z^\top \left(\frac{ZZ^\top}{N}\right)^{-1/2}, \tag{10}$$

where, based on Assumption 3, the second term on the right of (10) tends to zero with probability one (w.p.1) as N tends to infinity. That is

$$\lim_{N\to\infty} \frac{E_f Z^\top}{N} \left(\frac{ZZ^\top}{N}\right)^{-1/2} = 0. \tag{11}$$

Thus,

$$\lim_{N\to\infty} \frac{Z_f Z^\top}{N} \left(\frac{ZZ^\top}{N}\right)^{-1/2} = \lim_{N\to\infty} \frac{1}{N} \begin{bmatrix} \Gamma_f & H_f \\ 0 & I \end{bmatrix} \begin{bmatrix} X_f \\ U_f \end{bmatrix} Z^\top \left(\frac{ZZ^\top}{N}\right)^{-1/2}. \tag{12}$$

Since the following rank conditions hold (to be clarified in the proof of Theorem 1)

$$\begin{aligned} &rank\left(\lim_{N\to\infty}\frac{Z_f Z^\top}{N}\left(\frac{ZZ^\top}{N}\right)^{-1/2}\right)\\ &= rank\left(\begin{bmatrix}\Gamma_f & H_f\\ 0 & I\end{bmatrix}\right)\\ &= n_x + fn_u. \end{aligned} \tag{13}$$

The general estimates of Γ_f and H_f are then given by

$$\begin{bmatrix}\hat{\Gamma}_f & \hat{H}_f\\ 0 & I\end{bmatrix} = \hat{U}_1, \tag{14}$$

where $\hat{U}_1$ is obtained from a low-rank approximation using singular value decomposition (SVD)

$$\frac{Z_f Z^\top}{N}\left(\frac{ZZ^\top}{N}\right)^{-1/2} = [\hat{U}_1\ \hat{U}_2]\begin{bmatrix}\hat{S}_1 & 0\\ 0 & \hat{S}_2\end{bmatrix}\begin{bmatrix}\hat{V}_1^\top\\ \hat{V}_2^\top\end{bmatrix}, \tag{15}$$

where $\hat{S}_1 \in \Re^{(n_x+fn_u)\times(n_x+fn_u)}$, $\hat{U}_1 \in \Re^{f(n_u+n_y)\times(n_x+fn_u)}$, $\hat{V}_1^\top \in \Re^{(n_x+fn_u)\times p(n_u+n_y)}$, $\hat{S}_2 \in \Re^{(fny-n_x)\times(fn_y-n_x)}$, $\hat{U}_2 \in \Re^{f(n_u+n_y)\times(fn_y-n_x)}$, and $\hat{V}_2^\top \in \Re^{(fn_y-n_x)\times p(n_u+n_y)}$. We shall refer to these singular vectors of $\hat{U}_2$ and $\hat{V}_2^\top$ as the parity space or null space.

In this paper, Γ_f and H_f are estimated from the left parity space of $\frac{Z_f Z^\top}{N}\left(\frac{ZZ^\top}{N}\right)^{-1/2}$. By post-multiplying both sides of (14) with $\hat{U}_2^\top$ yields,

$$\hat{U}_2^\top\begin{bmatrix}\hat{\Gamma}_f & \hat{H}_f\\ 0 & I\end{bmatrix} = 0. \tag{16}$$

Denoting

$$\hat{U}_2^\top = [\hat{U}_{21}^\top, \hat{U}_{22}^\top], \tag{17}$$

where $\hat{U}_{21}^\top$ and $\hat{U}_{22}^\top$ are the first fn_y columns and the last fn_u columns of $\hat{U}_2^\top$, respectively. Substituting (17) into (16) yields

$$\hat{U}_{21}^\top\hat{\Gamma}_f = 0, \tag{18}$$

$$-\hat{U}_{21}^\top\hat{H}_f = \hat{U}_{22}^\top. \tag{19}$$

It follows from (18) that

$$\hat{\Gamma}_f = [\hat{U}_{21}^\top]^\perp, \tag{20}$$

where $[\hat{U}_{21}^\top]^\perp$ is a matrix for projection onto the orthogonal complement of the row space of $\hat{U}_{21}^\top$.

To estimate H_f, it is preferred to estimate $H_{f1} = [D^{\mathrm{T}}\ (CB)^{\mathrm{T}}\ldots(CA^{f-2}B)^{\mathrm{T}}]$ to avoid redundant computation. Letting

$$-\hat{U}_{21}^\top = [\phi_1\ldots\phi_f], \tag{21}$$

$$\hat{U}_{22}^\top = [\varphi_1\ldots\varphi_f], \tag{22}$$

where $\phi_i \in \Re^{(in_y-n_x)\times n_y}$ and $\varphi_i \in \Re^{(in_y-n_x)\times n_u}$ for $i = 1,\ldots,f$.

Substituting (21) and (22) into (19) yields

$$[\phi_1\ldots\phi_f]\hat{H}_{f1} = [\varphi_1\ldots\varphi_f]. \tag{23}$$

It follows that

$$\xi\hat{H}_{f1} = \eta, \tag{24}$$

where

$$\eta = \begin{bmatrix}\phi_1 & \ldots & \phi_{f-1} & \phi_f\\ \phi_2 & \ldots & \phi_f & 0\\ \vdots & \vdots & \ddots & \vdots\\ \phi_f & 0 & \vdots & 0\end{bmatrix}, \tag{25}$$

$$\xi = [\varphi_1\ldots\varphi_f]^\top. \tag{26}$$

A least squares (LS) solution to $\hat{H}_{f1}$ is then obtained as

$$\hat{H}_{f1} = \xi^\dagger\eta. \tag{27}$$

3.2. Estimation of system matrices

The matrices $\hat{C}$ and $\hat{A}$ can be extracted directly from $\hat{\Gamma}_f$ as follows:

$$\hat{C} = \hat{\Gamma}(1:n_y, 1:n_x), \tag{28}$$

$$\hat{\Gamma}_f(n_x+1:fn_y,:) = \hat{\Gamma}_f(1:(f-1)n_y,:)\hat{A}, \tag{29}$$

where Matlab notation is used for partitioning matrices. Therefore, a LS solution of $\hat{A}$ is obtained as

$$\hat{A} = \hat{\Gamma}_f^\dagger(1:(f-1)n_y,:)\hat{\Gamma}_f(n_x+1:fn_y,:). \tag{30}$$

The matrices $\hat{B}$ and $\hat{D}$ can then be extracted directly from $\hat{H}_{f1}$ along with $\hat{C}$ and $\hat{A}$. It follows from $\hat{H}_{f1}$ that

$$H_{f1} = \begin{bmatrix}I_{n_y} & 0\\ 0 & \Gamma(1:(f-1)n_y, 1:n_x)\end{bmatrix}\begin{bmatrix}D\\ B\end{bmatrix}. \tag{31}$$

Therefore, a LS solutions of $\hat{B}$ and $\hat{D}$ are obtained as

$$\begin{bmatrix}\hat{D}\\ \hat{B}\end{bmatrix} = \begin{bmatrix}I_{n_y} & 0\\ 0 & \hat{\Gamma}(1:(f-1)n_y, 1:n_x)\end{bmatrix}^\dagger\hat{H}_{f1}. \tag{32}$$

The improved subspace identification method using parity space (SIMps) can be summarized as follows:

Input: Sampled input-output data; Past and future horizons p and f; System order n_x.
Output: System matrices A, B, C, D
Step 1: Eliminate the noise term as (10);
Step 2: Perform SVD as (15);
Step 3: Estimate Γ_f and H_{f1} as (20) and (27);
Step 4: Estimate A, B, C, D as (28), (30) and (32).

4. CONSISTENT ANALYSIS

As is well-known in [11–13] that to obtain consistent estimates of system matrices (A,B,C,D), the rank conditions in (13) must be strictly fulfilled. The explicit conditions on the input signals and on the system for consistency of SIMps are then established by analyzing the rank conditions in (13), as stated in the following theorem. Before analying the consistency of SIMps, the following Lemmas are first given.

Lemma 1 [32]**:** For matrices $X_1 \in \Re^{m\times n}$ and $X_2 \in \Re^{n\times r}$, the following rank conditions hold

1) $rank(X_1) \le min(m,n)$,

2) $rank(X_1) + rank(X_2) - n \le rank(X_1X_2) \le min(rank(X_1), rank(X_2))$,

3) $rank(X_1) \le rank(X_1^\top)$.

Lemma 2 [7]**:** For matrices $X_1 \in \Re^{m\times m}$, $X_2 \in \Re^{n\times n}$, $X_3 \in \Re^{n\times m}$, and a non-singular matrix $X_4 \in \Re^{n\times n}$, and the block-matrix

$$W = \begin{bmatrix} X_1 & X_2 \\ X_3 & X_4 \end{bmatrix} \in \Re^{(m+n)\times(m+n)}. \tag{33}$$

Then,

$$rank(W) = n + rank(X_1 - X_2X_4^{-1}X_3). \tag{34}$$

Theorem 1: SIMps is consistent if the general Assumptions 1-3 and the following conditions hold

1) The input signal is persistently exciting (PE) of order $n+p+f$;

2) $p \ge n_x$ and $f \ge n_x$.

Proof: By substituting (7) into the left side of (13) yields

$$\begin{aligned} &rank\left(\lim_{N\to\infty}\frac{Z_fZ^\top}{N}\left(\frac{ZZ^\top}{N}\right)^{-1/2}\right) \\ &= rank\left(\lim_{N\to\infty}\frac{1}{N}\begin{bmatrix}\Gamma_f & H_f\end{bmatrix}\begin{bmatrix}X_f\\U_f\end{bmatrix} + \begin{bmatrix}I\\0\end{bmatrix}E_f\begin{bmatrix}Y_p\\U_p\\U_f\end{bmatrix}^\top \Xi\right), \end{aligned} \tag{35}$$

where $\Xi = \left(\frac{1}{N}\begin{bmatrix}Y_p\\U_p\\U_f\end{bmatrix}\begin{bmatrix}Y_p\\U_p\\U_f\end{bmatrix}^\top\right)^{-1/2}$. Since that the input and noise are jointly stationary and uncorrelated with each other, (35) can be rewritten as

$$\begin{aligned} &rank\left(\lim_{N\to\infty}\frac{Z_fZ^\top}{N}\left(\frac{ZZ^\top}{N}\right)^{-1/2}\right) \\ &= rank\left(\begin{bmatrix}\Gamma_f & H_f\\0 & I\end{bmatrix}\lim_{N\to\infty}\left(\frac{1}{N}\begin{bmatrix}X_f\\U_f\end{bmatrix}\begin{bmatrix}Y_p\\U_p\\U_f\end{bmatrix}^\top\right)\left(\frac{\Xi}{N}\right)\right). \end{aligned} \tag{36}$$

If $f \ge n_x$, based on Assumption 2,

$$rank(\Gamma_f) = n_x. \tag{37}$$

In view of Lemma 2, the rank of the first factor at the right side of (36) can be computed as follows

$$rank\left(\begin{bmatrix}\Gamma_f & H_f\\0 & I\end{bmatrix}\right) = rank(\Gamma_f) + fn_u = n_x + fn_u. \tag{38}$$

According to the statement (1) in Lemma 1, we have

$$rank\left(\lim_{N\to\infty}\left(\frac{1}{N}\begin{bmatrix}X_f\\U_f\end{bmatrix}\begin{bmatrix}Y_p\\U_p\\U_f\end{bmatrix}^\top\right)\left(\frac{\Xi}{N}\right)\right) \le n_x + fn_u. \tag{39}$$

In view of the statement (2) in Lemma 1, the conditions (13) hold if and only if

$$rank\left(\lim_{N\to\infty}\left(\frac{1}{N}\begin{bmatrix}X_f\\U_f\end{bmatrix}\begin{bmatrix}Y_p\\U_p\\U_f\end{bmatrix}^\top\right)\left(\frac{\Xi}{N}\right)\right) = n_x + fn_u. \tag{40}$$

By substituting (6), (7) and (8) into (40), the condition in (40) is equivalent to

$$\begin{aligned} &rank\left(\begin{bmatrix}A^p & L_p & 0\\0 & 0 & I\end{bmatrix}\lim_{N\to\infty}\left(\frac{\Xi_1}{N}\right)\begin{bmatrix}\Gamma_p & H_p & 0\\0 & I & 0\\0 & 0 & I\end{bmatrix}^\top\right. \\ &\left.\times\begin{bmatrix}\Gamma_p & H_p & 0\\0 & I & 0\\0 & 0 & I\end{bmatrix}\lim_{N\to\infty}\left(\frac{\Xi_1}{N}\right)\begin{bmatrix}\Gamma_p & H_p & 0\\0 & I & 0\\0 & 0 & I\end{bmatrix}^\top\right) \\ &= n_x + fn_u, \end{aligned} \tag{41}$$

where $\Xi_1 = \left(\frac{1}{N}\begin{bmatrix}X_p\\U_p\\U_f\end{bmatrix}\begin{bmatrix}X_p\\U_p\\U_f\end{bmatrix}^\top\right)$. The first factor at the right side of (41) has full row rank of $fn_u + n_x$ if the system (1) is reachable from $u(t)$ and if $p \ge n_x$, that is

$$rank\left(\begin{bmatrix}A^p & L_p & 0\\0 & 0 & I\end{bmatrix}\right) = n_x + fn_u. \tag{42}$$

The second factor at the right side of (41) has full row rank if input is PE of order $p+f+n_x$. Then,

$$rank\left(\lim_{N\to\infty}\Xi_1\right) = n_x + fn_u. \tag{43}$$

The third factor at the right side of (41) is full row rank of $n_x + (p+f)n_u$ if $p \ge n_x$ along with the statement (3) in Lemma 1 and Lemma 2, that is

$$rank\left(\begin{bmatrix}\Gamma_p & H_p & 0\\0 & I & 0\\0 & 0 & I\end{bmatrix}\right) = n_x + (p+f)n_u. \tag{44}$$

Table 1. Overview of different IVs for different algorithms.

Algorithms	IVs
SIMps	$Z^\top (ZZ^\top/N)^{-1/2}$
SIMPCA [11]	$Z_p^\top$
SIMPCA-Wc [13]	$Z_p^\top (Z_p Z_p^\top/N)^{-1/2}$

Combining (42), (43), and (44), it is obvious that the rank conditions in (13) hold under the conditions as summarized in Theorem 1. This completes the proof. □

Remark 1: For clarity the presentation of the main idea, we only study systems subject to measurement noises. Extending SIMps to systems with both measurement/process noises does not change of the arguments of the paper generally at least if $pn_u \geq n_x$ [7].

Remark 2: The three algorithms (SIMps, SIMPCA [12], and SIMPCA-Wc [13]) identify the system matrices under the same algorithm framework, but each uses a different IV, see Table 1 for more details. These IVs are all uncorrelated with noise, but the IV in SIMps including the future data is maximally correlated with than other IVs.

Remark 3: To get consistent estimations of Γ_f and H_f, the following rank condition must be fulfilled for SIMPCA and SIMPCA-Wc as pointed in [11].

$$rank\left(\lim_{N\to\infty}\frac{Z_f Z_p^\top}{N}\right) = n_x + fn_u. \tag{45}$$

Substituting (6), (7), and (8) into (45), we have

$$\begin{aligned} &rank\left(\lim_{N\to\infty}\frac{Z_f Z_p^\top}{N}\right) \\ &= rank\left(\begin{bmatrix}\Gamma_f & H_f\\ 0 & I\end{bmatrix}\begin{bmatrix}A^p & L_p & 0\\ 0 & 0 & I\end{bmatrix}\lim_{N\to\infty}\left(\frac{\Xi_1}{N}\right)\right. \\ &\quad\left.\times\begin{bmatrix}\Gamma_p & H_p & 0\\ 0 & I & 0\\ 0 & 0 & 0\end{bmatrix}^\top\right). \end{aligned} \tag{46}$$

Under the assumed conditions shown in Theorem 1, the rank of the previous three factors in (46) can be computed as (42), (38), and (43), which are equivalent to $n_x + fn_u$, $n_x + fn_u$, and $n_x + (p+f)n_u$, respectively. The rank of the last factor in (46) along with Lemma 2 is $n_x + pn_u$.Then, (46) along with the statement (2) in Lemma 1 is

$$\begin{aligned} n_x &\leq rank\left(\lim_{N\to\infty}\frac{Z_f Z_p^\top}{N}\right) \\ &\leq min(n_x + fn_u, n_x + pn_u). \end{aligned} \tag{47}$$

Its obviously that the rank condition for consistency of SIMPCA and SIMPCA-Wc may not be fulfilled.

Remark 4: For linear/nonlinear systems with nonGaussian noises, output constraints, outliers-in-measurements, and error-in-variables which are common in practical applications, the proposed method may not guarantee consistent estimations. These issues have been considered in the recent references [19, 20, 33–35], and deserves further exploration in our future work.

5. ILLUSTRATION

In this section, we use two examples to evaluate the proposed SIMps method and compare it with the SIMPCA [11, 12] and SIMPCA-Wc methods [13].

Example 1: The following second-order system is the nominal model for numerical simulation study [11, 36]:

$$\begin{cases} x(t+1) = Ax(t) + Bu(t), \\ y(t) = Cx(t) + Du(t) + v(t), \end{cases}$$

where

$$A = \begin{bmatrix} 0.67 & 0.67 & 0 & 0 \\ -0.67 & 0.67 & 0 & 0 \\ 0 & 0 & -0.67 & -0.67 \\ 0 & 0 & 0.67 & 0.67 \end{bmatrix},$$

$$B = \begin{bmatrix} 0.6598 & 1.9698 & 4.3171 & -2.6436 \end{bmatrix}^\top,$$

$$C = \begin{bmatrix} -0.5749 & 1.0751 & -0.5225 & 0.1830 \end{bmatrix},$$

and $D = -0.7139$.

The noises are white, Gaussian, and zero-mean, with variance of σ^2. The parameters are chosen as $p = f = 7$, and both colored and white signals are used as the input excitation.

Case 1 (Colored input): The input is a combination of 10 sine waves with different frequencies $u(t) = \sum_{j=1}^{10} sin(0.3898pjk)$. We investigate the effectiveness and merit of SIMps under different noise variances $\sigma^2 = 0.1, 0.3$. For illustration, a Monte-Carlo (MC) test of fifty runs is performed with 500 data points for each run. Fig. 1 shows a comparison of computed singular values of $\frac{Z_f Z^\top}{N}\left(\frac{ZZ^\top}{N}\right)^{-1/2}$, $\frac{Z_f Z_p^\top}{N}$, and $\frac{Z_f Z_p^\top}{N}\left(\frac{Z_p Z_p^\top}{N}\right)^{-1/2}$ in the SIMPCA, SIMPCA-Wc and SIMps methods. Since the singular values in all methods decline quickly when the order is larger than 12, it can be concluded that $fn_u + n_x = 11$. These methods provide consistent estimated results.

Fig. 2 shows a comparison of the poles of A estimated by using different methods. More details about the mean and variance of the estimated poles are demonstrated in Table 2. Further, the Bode magnitude plots of the obtained models are shown in Fig. 3, which are calculated by the bode command in the Matlab System Identification Toolbox. Due to the IVs in these methods are correlated with the future input data for colored input, all of the identified poles and Bode magnitude are consistent. Moreover,

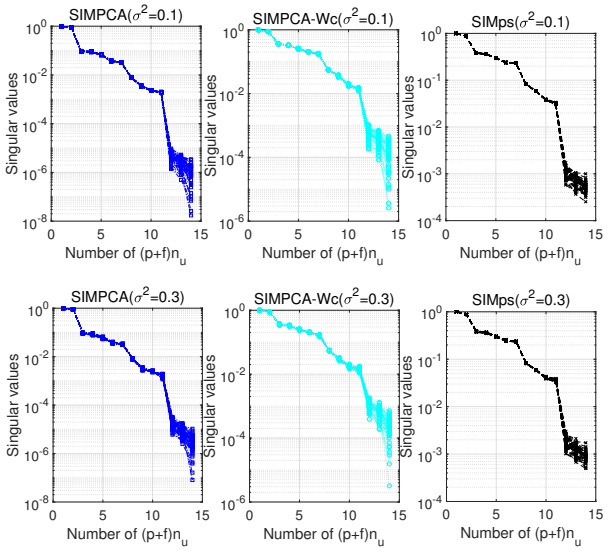

Fig. 1. Comparison of computed singular values using different methods for Case 1.

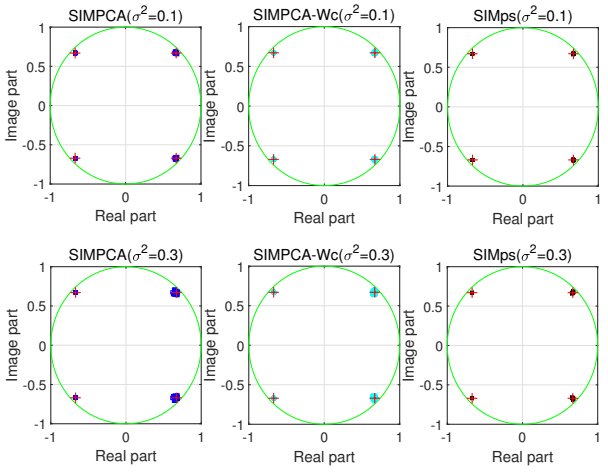

Fig. 2. Comparison of estimated poles using different methods for Case 1. (red "+": true value).

Table 2. Identified poles using different algorithms for Case 1.

Methods	σ^2	True poles	
		-0.6700±0.6700i	0.6700±0.6700i
SIMPCA	0.1	-0.6700(±0.005)± 0.6674i(±0.0042)	0.6697(±0.0069)± 0.6737i(±0.0050)
SIMPCA-Wc	0.1	-0.6700(±0.0005)± 0.6672i(±0.0043)	0.6709(±0.0059)± 0.6740i(±0.0050)
SIMps	0.1	-0.6700(±0.0004) ±0.6680i(±0.0023)	0.6702(±0.0041)± 0.6721i(±0.0032)
SIMPCA	0.3	-0.6700(±0.0008)± 0.6635i(±00096)	0.6610(±0.0168)± 0.6775i(±0.0102)
SIMPCA-Wc	0.3	-0.6700(±0.0008)± 0.6644)i(±0.0081)	0.6643(±0.0115)± 0.6753)i(±0.0086)
SIMps	0.3	-0.6700(±0.0006)± 0.6672i(±0.0042)	0.6691(±0.0065)± 0.6733i(±0.0056)

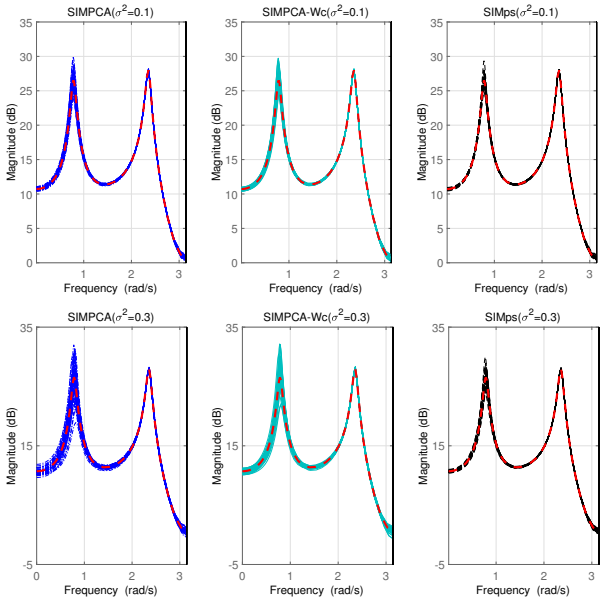

Fig. 3. Bode magnitude plots using different methods for Case 1. (red: true value).

it can be seen that SIMps results in a slight smaller variance compared to SIMPCA and SIMPCA-Wc under the same noises variances.

Case 2 (White noise input): The input is chosen as a zero-mean white Gaussian noise with unit variance. Several noises variances $\sigma^2 = 0.1,\ 0.3$ are chosen to better show the effectiveness and merit of SIMps. Fifty MC tests are performed with 500 data points for each noise variances. A comparison of computed singular values in these methods are shown in Fig. 4. It can be seen that the singular value in SIMps obviously falls off a cliff with order 12, but this value in SIMPCA and SIMPCA-Wc is only 5. The SIMPCA and SIMPCA-Wc methods lead to a loss in the rank of the future input/output Hankel matrix, thus SIMPCA and SIMPCA-Wc may yield biased estimates. Fig. 5 shows a comparison of poles estimated using these methods. A straight comparison of the mean and variance from the estimation of these poles are demonstrated in Table 3. Fig. 6 shows the identified Bode magnitude plots. Due to that only the new IV in SIMps is correlated with the future input data for white input, the proposed IV is more correlated with than the other IVs in SIMPCA and SIMPCA-Wc. It can be seen from Figs. 5 and 6 and Table 3 that the proposed method generally enhances the estimated model efficiency/accuracy compared to SIMPCA and SIMPCA-Wc under same noise variances.

Example 2: Consider an injection moulding process

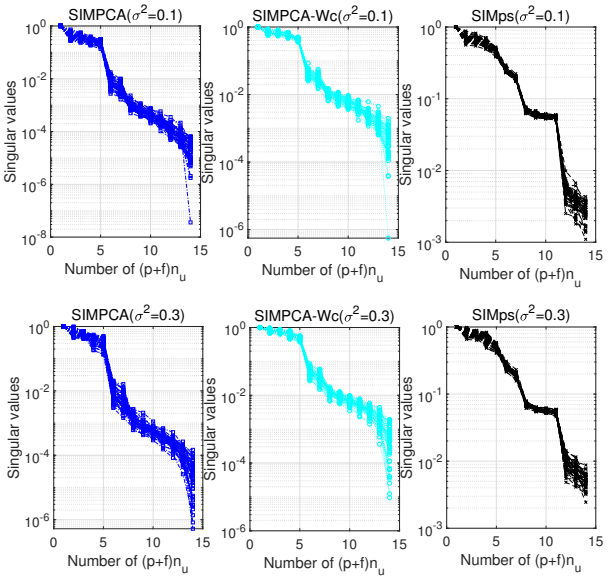

Fig. 4. Comparison of computed singular values using different methods for Case 2.

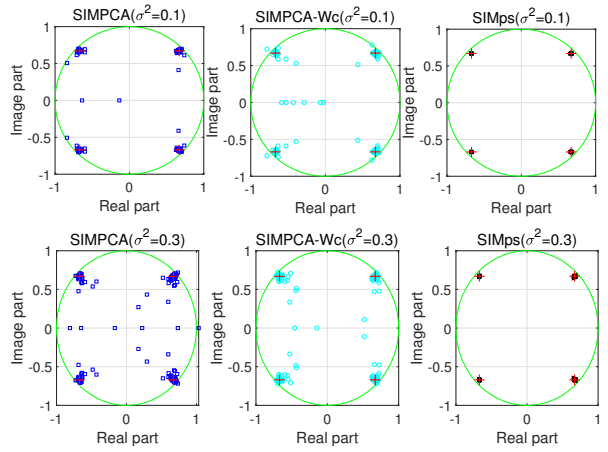

Fig. 5. Comparison of estimated poles using different methods for Case 2. (red "+": true value).

studied in the references [37,38]:

$$\begin{cases} x(t+1) = \begin{bmatrix} 1.2810 & -0.5916 \\ 1 & 0 \end{bmatrix} x(t) + [1,0]^\top u(t), \\ y(t) = [1.69, 1.419]x(t) + v(t). \end{cases}$$

The input excitation is a weakly correlated signal:

$$u(t) = (1 + 0.8q^{-1} + 0.6q^{-2})u_0(t),$$

where $u_0(t)$ is a PBRS signal with mean value 0.5 and variance 0.4. The noises are assumed to Gaussian white with zero-mean and variance of 0.1. Fifty MC tests are performed with 9000 data points. Fig. 7 shows a comparison of poles estimated by using these methods and Fig. 8

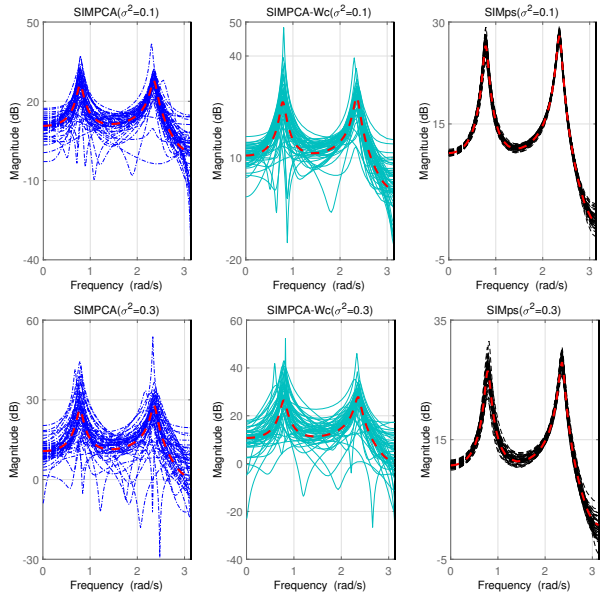

Fig. 6. Bode magnitude plots using different methods for Case 2. (red: true value).

Table 3. Identified poles using different algorithms for Case 2.

Methods	σ^2	True poles	
		-0.6700±0.6700i	0.6700±0.6700i
SIMPCA	0.1	-0.6713(±0.0308)± 0.6410i(±0.0097)	0.6708(±0.0172)± 0.6759i(±0.1023)
SIMPCA-Wc	0.1	-0.6293(±0.0619)± 0.6152i(±0.1593)	0.6661(±0.0375)± 0.6725i(±0.0318)
SIMps	0.1	-0.6703(±0.0037) ±0.6664i(±0.0038)	0.6703(±0.0067)± 0.6743i(±0.0329)
SIMPCA	0.3	-0.6602(±0.1917)± 0.6002i(±0.1584)	0.6599(±0.0553)± 0.6743i(±0.0329)
SIMPCA-Wc	0.3	-0.6470(±0.0658)± 0.6270)i(±0.1125)	0.6644(±0.0379)± 0.6765i(±0.0337)
SIMps	0.3	-0.6695(±0.0061)± 0.6659i(±0.0069)	0.6708(±0.0085)± 0.6753i(±0.0069)

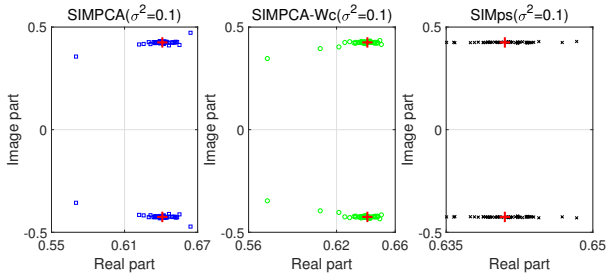

Fig. 7. Comparison of estimated poles using different methods for Example 2. (red "+": true value).

shows the identified Bode magnitude plots. A straight comparison of the mean and variance from the estimation

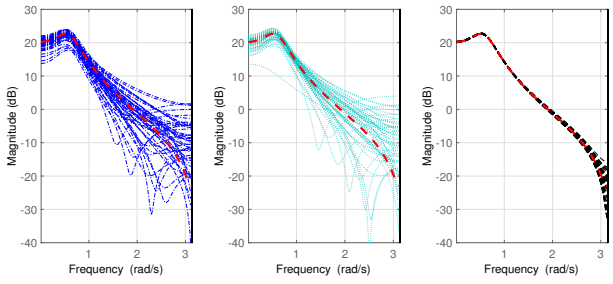

Fig. 8. Bode magnitude plots using different methods for Example 2. (red: true value).

Table 4. Identified poles using different algorithms for Example 2.

True poles	$0.6410 \pm 0.4251i$
SIMPCA	$0.6406(\pm 0.0084) \pm 0.4242(\pm 0.0060)i$
SIMPCA-Wc	$0.6407(\pm 0.0117) \pm 0.4257(\pm 0.0326)i$
SIMps	$0.6408(\pm 0.0026) \pm 0.4248(\pm 0.0017)i$

of these poles are demonstrated in Table 4.

While the identified poles and Bode magnitude are consistent, the SIMps algorithm results in a smaller variance of the estimated Bode magnitude compared to SIMPCA and SIMPCA-Wc. It is again seen that the SIMps method enhances identification accuracy compared to SIMPCA and SIMPCA-Wc.

6. CONCLUSION

A consistent subspace method using parity space, SIMps, has been developed in the same framework with SIMPCA and SIMPCA-Wc, in which a new IV which consists of the future/past input data and past output data was used to eliminate the noise effect. Since the new IV is highly correlated with the future data but uncorrelated with the noise, the rank conditions for consistent estimation of the extended observability matrix and the triangular block-Toeplitz matrix can be fulfilled. Therefore, the SIMps method can provide consistent estimates. However, the IVs in SIMPCA and SIMPCA-Wc are constructed by only the past input /output data, which are uncorrelated with the future input data for white input systemsbut weakly correlated with the future input data for colored input systems. The rank conditions for consistent estimations of the extended observability matrix and the triangular block-Toeplitz matrix may not fulfilled strictly. As a consequence, SIMPCA and SIMPCA-Wc may yield a biased solution, especially, for white input systems. The main merit of SIMps is that it can enhance the estimated model efficiency/accuracy compared to SIMPCA and SIMPCA-Wc, as supported by the rank condition analysis and two numerical examples presented in the previous sections of this paper.

REFERENCES

[1] P. V. Overschee and B. L. De Moor, *Subspace Identification for Linear Systems: Theory-implementation-applications*, Springer, Berlin, 2012.

[2] T. Katayama, *Subspace Methods for System Identification*, Springer, Berlin, 2006.

[3] S. J. Qin, "An overview of subspace identification," *Computers & Chemical Engineering*, vol. 30, no. 10-12, pp. 1502-1513, September 2006.

[4] M. Verhaegen, "Identification of the deterministic part of MIMO state-space models given in innovations form from input-output data," *Automatica*, vol. 30, no. 1, pp. 61-74, January 1994.

[5] W. E. Larimore, "System identification, reduced-order filtering and modeling via canonical variate analysis," *American Control Conference*, pp. 445-451, June 1983.

[6] P. V. Overschee and B. L. De Moor, "N4SID: subspace algorithms for the identification of combined deterministic-stochastic systems," *Automatica*, vol. 30, no. 1, pp. 75-93, January 1994.

[7] M. Jansson and B. Wahlberg, "On consistency of subspace methods for system identification," *Automatica*, vol. 34, no. 12, pp. 1507-1519, December 1998.

[8] A. Chiuso and G. Picci, "The asymptotic variance of subspace estimates," *Journal of Econometrics*, vol. 118, no. 1-2, pp. 257-291, JanuaryFebruary 2004.

[9] D. Bauer, "Estimating ARMAX systems for multivariate time series using the state approach to subspace algorithms," *Journal of Multivariate Analysis*, vol. 100, no. 3, pp. 397-421, March 2009.

[10] J. Hou, T. Liu, and F. Chen, "Orthogonal projection based subspace identification against colored noise," *Control Theory and Technology*, vol. 15, no. 1, pp. 69-77, February 2017.

[11] W. Li and S. J. Qin, "Consistent dynamic PCA based on errors-in-variables subspace identification," *Journal of Process Control*, vol. 11, no. 6, pp. 661-678, December 2001.

[12] J. Wang and S. J. Qin, "A new subspace identification approach based on principal component analysis," *Journal of Process Control*, vol. 12, no. 8, pp. 841-855, December 2002.

[13] J. Wang and S. J. Qin, "Closed-loop subspace identification using the parity space," *Automatica*, vol. 42, no. 2, pp. 315-320, February 2006.

[14] W. Li, H. Raghavan, and S. Shah, "Subspace identification of continuous time models for process fault detection and isolation," *Journal of Process Control*, vol. 13, no. 5, pp. 407-421, August 2003.

[15] A. Micchi and G. Pannocchia, "Comparison of input signals in subspace identification of multivariable ill-conditioned systems," *Journal of Process Control*, vol. 18, no. 6, pp. 582-593, July 2008.

[16] H. Yang, S. Li, and K. Li, "Order estimation of multivariable ill-conditioned processes based on PCA method," *Journal of Process Control*, vol. 22, no. 7, pp. 1397-1403, August 2012.

[17] Z. Liao, Z. Zhu, S. Liang, C. Peng, and Y. Wang, "Subspace identification for fractional order Hammerstein systems based on instrumental variables," *International Journal of Control, Automation and Systems*, vol. 10, no. 5, pp. 947-953, September 2012.

[18] P. Wu, H. P. Pan, J. Ren, and C. Yang, "A new subspace identification approach based on principal component analysis and noise estimation," *Industrial & Engineering Chemistry Research*, vol. 54, no. 18, pp. 5106-5114, April 2015.

[19] D. Maurya, A. K. Tangirala, and S. Narasimhan, "Identification of Errors-in-Variables models using dynamic iterative principal component analysis," *Industrial & Engineering Chemistry Research*, vol. 57, no. 35, pp. 11939-11954, August 2018.

[20] J. Hou, T. Liu, B. Wahlberg, and M. Jansson, "Subspace Hammerstein model identification under periodic disturbance," *IFAC-PapersOnLine*, vol. 51, no. 15, pp. 335-340, July 2018.

[21] S. X. Ding, P. Zhang, A. Naik, E. L. Ding, and B. Huang, "Subspace method aided data-driven design of fault detection and isolation systems," *Journal of Process Control*, vol. 19, no. 9, pp. 1496-1510, October 2009.

[22] S. X. Ding, "Data-driven design of monitoring and diagnosis systems for dynamic processes: a review of subspace technique based schemes and some recent results," *Journal of Process Control*, vol. 24, no. 2, pp. 431-449, February 2014.

[23] S. Yin, G. Wang, and H. R. Karimi, "Data-driven design of robust fault detection system for wind turbines," *Mechatronics*, vol. 24, no. 4, pp. 298-306, June 2014.

[24] S. Yin, S. X. Ding, X. Xie, and H. Luo, "A review on basic data-driven approaches for industrial process monitoring," *IEEE Transactions on Industrial Electronics*, vol. 61, no. 11, pp. 6418-6428, November 2014.

[25] S. Yin, S. X. Ding, A. H. Abandan Sari, and H. Hao, "Data-driven monitoring for stochastic systems and its application on batch process," *International Journal of Systems Science*, vol. 44, no. 7, pp. 1366-1376, July 2013.

[26] K. Peng, M. Wang, and J. Dong, "Event-triggered fault detection framework based on subspace identification method for the networked control systems," *Neurocomputing*, vol. 239, no. 24, pp. 257-267, May 2017.

[27] G. Wang and Z. Huang, "Data-driven fault-tolerant control design for wind turbines with robust residual generator," *IET Control Theory & Applications*, vol. 9, no. 7, pp. 1173-1179, April 2015.

[28] J. S. Wang and G. H. Yang, "Data-driven output-feedback fault-tolerant compensation control for digital PID control systems with unknown dynamics," *IEEE Transactions on Industrial Electronics*, vol. 63, no. 11, pp. 7029-7039, November 2016.

[29] Y. Wang, H. Zhang, S. Wei, D. Zhou, and B. Huang, "Control performance assessment for ILC-controlled batch processes in a 2-D system framework," *IEEE Transactions on Systems, Man, and Cybernetics: Systems*, vol. 48, no. 9, pp. 1493-1504, September 2017.

[30] J. S. Wang and G. H. Yang, "Data-driven compensation method for sensor drift faults in digital PID systems with unknown dynamics," *Journal of Process Control*, vol. 65, pp. 15-33, May 2018.

[31] H. Oku and H. Kimura, "A recursive 4SID from the input-output point of view," *Asian Journal of Control*, vol. 1, no. 4, pp. 258-269, December 1999.

[32] D. S. Bernstein, *Matrix Mathematics*, 2nd ed., Princeton University Press, Princeton, 2009.

[33] V. Filipovic, N. Nedic, and V. Stojanovic, "Robust identification of pneumatic servo actuators in the real situations," *Forschung im Ingenieurwesen*, vol. 75, no. 4, pp. 183-196, December 2011.

[34] V. Stojanovic and N. Nedic, "Robust identification of OE model with constrained output using optimal input design," *Journal of the Franklin Institute*, vol. 353, no. 2, pp. 576-593, January 2016.

[35] V. Stojanovic and N. Nedic, "Joint state and parameter robust estimation of stochastic nonlinear systems," *International Journal of Robust and Nonlinear Control*, vol. 26, no. 14, pp. 3058-3074, September 2016.

[36] P. V. Overschee and B. L. De Moor, "A unifying theorem for three subspace system identification algorithms," *Automatica*, vol. 31, no. 12, pp. 1853-1864, December 1995.

[37] T. Liu, B. Huang, and S. J. Qin, "Bias-eliminated subspace model identification under time-varying deterministic type load disturbance," *Journal of Process Control*, vol. 25, pp. 41-49, January 2015.

[38] J. Hou, T. Liu, and Q. G. Wang, "Recursive subspace identification subject to relatively slow time-varying load disturbance," *International Journal of Control*, vol. 91, no. 3, pp. 648-664, May 2018.

Jie Hou received his Ph.D. degree in Control Theory and Control engineering from Dalian University of Technology in 2018. His research interests include process modelling and system identification.

Fengwei Chen received his Ph.D. degree from Universite de Lorraine in 2014. His research interests include system identification and signal processing.

Penghua Li received his Ph.D. degree in Control Theory and Control engineering from Chongqing University in 2012. His research interest includes fault diagnosis.

Zhiqin Zhu received his Ph.D. degree in Control Theory and Control engineering from Chongqing University in 2017. His research interests include image processing and identification.

Fei Liu received his Ph.D. degree in Control theory and Control engineering from Chongqing University in 2015. His research interests include intelligent mobile robot control, navigation, robot testing and assessment.